Chain structure and electronic states of liquid Rb-Se mixtures by *ab initio* molecular-dynamics simulations

Fuyuki Shimojo
Department of Physics, Kumamoto University, Kumamoto 860-8555, Japan

Kozo Hoshino
Graduate School of Integrated Arts and Sciences, Hiroshima University, Higashi-Hiroshima 739-8521, Japan
(Received 9 June 2006; published 18 September 2006)

The effects of excess electronic charges transferred from alkali metals to Se atoms on the chain structure in liquid Rb_xSe_{1-x} for $x \leqslant 0.5$ are investigated by means of *ab initio* molecular-dynamics simulations. It is found that the interaction between Se chains is enhanced by the transferred electrons, and that the average length of Se chains becomes shorter with increasing alkali-metal concentration. The shortening of Se chains is responsible for an increase of electronic states at the Fermi level, which explains the observed increase of the electrical conductivity on the addition of alkali metals. At the equiatomic concentration, there are almost no electronic states at the Fermi level due to the formation of Se_2^{2-} dimers. The alkali-metal-concentration dependence of the bonding properties between Se atoms is discussed in comparison with liquid alkali-metal tellurides based on a population analysis.

DOI: 10.1103/PhysRevB.74.104202 PACS number(s): 61.20.Ja, 71.22.+i, 71.15.Pd

I. INTRODUCTION

Liquid Se has a chain structure of covalently bonded atoms in twofold coordination.[1] Each chain molecule includes 10^5 atoms on the average near the triple point.[2,3] In a wide range of pressure and temperature, liquid Se exhibits semiconducting behavior similar to that of the crystalline phase. It is known, however, that the electronic properties become metallic, accompanied by a shortening of Se chains under high pressures and high temperatures near the critical point.[4,5] In the metallization process, bond breaking induced by interchain interaction plays an important role, together with the electronic states that have large amplitudes of wave functions near the ends of chains.[6]

In contrast to liquid Se, liquid Te exhibits semimetallic properties on melting, while the crystalline phase is a typical semiconductor. Although the chain structure is loosely preserved in the liquid phase, there exist many threefold-coordinated Te atoms.[7–9] It has been considered that the metallic properties of liquid Te arise from these coordination defects.

The effects of the addition of alkali metals on the electronic and structural properties of liquid Te have been extensively studied by both experimental[10–15] and theoretical[16–18] methods so far. With increasing alkali-metal concentration, the electrical conductivity decreases monotonically,[10–12] i.e., the electrical conductivity of pure liquid Te is about 2000 $\Omega^{-1}\,\mathrm{cm}^{-1}$, and it is only about 1 $\Omega^{-1}\,\mathrm{cm}^{-1}$ at an alkali-metal concentration of 50%. It has been suggested that the disappearance of the metallic properties in liquid alkali-metal tellurides is closely related to the stabilization of the chain structure due to excess electronic charges transferred from alkali metals to Te atoms.[16,17]

It is experimentally known that the electrical conductivity increases on the addition of alkali metals in liquid Se,[19,20] as opposed to the behavior of liquid Te. If the chain structure of liquid Se was stabilized by the transferred electrons, the electrical conductivity would decrease in the same way as in the liquid alkali-metal–Te mixtures. It is interesting to consider such contradicting alkali-metal-concentration dependence of the electronic properties in relation to the chain structure of the liquid alkali-metal–chalcogen mixtures. Recently, the structure of liquid Rb-Se mixtures has been investigated by extended x-ray absorption fine structure and neutron diffraction experiments.[21,22] It was found that the structure factor $S(k)$ has a small prepeak at about $k=1.3$ Å^{-1}. The spatial correlation between Se chains and Rb atoms was discussed based on the experimental results together with reverse Monte Carlo simulations. It was concluded that the prepeak is associated with an interchain correlation. However, the microscopic origin of the increase of the electrical conductivity due to the addition of alkali metals is still unknown.

In this study, we investigate the structure and electronic states of liquid Rb-Se mixtures by *ab initio* molecular-dynamics simulations. The purposes of our simulations are to clarify the effects of excess electronic charges transferred from alkali metals to Se atoms on the chain structure, and to discuss the bonding properties between Se atoms in liquid alkali-metal selenides in comparison with those between Te atoms in liquid alkali-metal tellurides.[16,17]

II. METHOD OF CALCULATION

The electronic structure calculations were performed within the framework of the density functional theory, in which the generalized gradient approximation[23] was used for the exchange-correlation energy. The electronic wave functions and the electron density were expanded in plane-wave basis sets with cutoff energies of 11 and 65 Ry, respectively. The energy functional was minimized using an iterative scheme based on the preconditioned conjugate-gradient method.[24,25] Ultrasoft pseudopotentials[26] were utilized for the interactions between valence electrons and ions. The molecular-dynamics simulations were carried out at three Rb

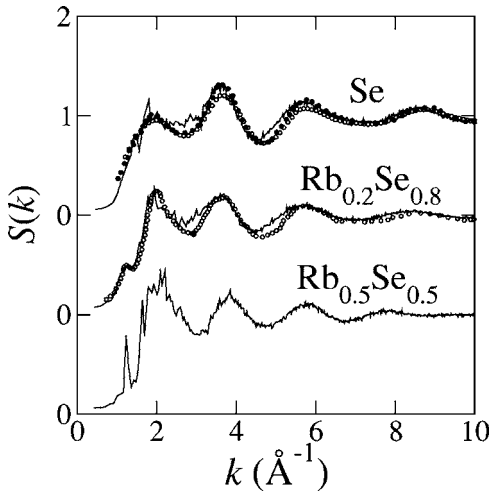

FIG. 1. Structure factors $S(k)$ of liquid Rb_xSe_{1-x}. The calculated results (solid lines) are compared with the experimental $S(k)$'s obtained by x-ray diffraction measurements at 300 °C and 12 bar of Tamura and Hosokawa (Ref. 29) (open circles) for $x=0.0$, x-ray diffraction measurements at 300 °C and 9.8 bar of Tamura and Inui (Ref. 30) (solid circles) for $x=0.0$, and neutron diffraction measurements at 280 °C and 1 bar of Maruyama *et al.* (Ref. 22) (open circles) for $x=0.2$.

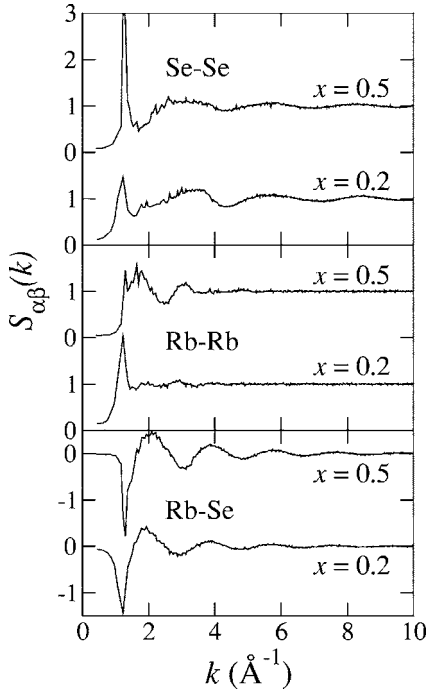

FIG. 2. Ashcroft-Langreth partial structure factors $S_{\alpha\beta}(k)$ of liquid Rb_xSe_{1-x}.

concentrations: Rb_xSe_{1-x} with $x=0.0$, 0.2, and 0.5. For each Rb concentration, we used an 80-atom system in a cubic supercell with periodic boundary conditions. The temperatures and number densities are (560 K, 0.0294 Å^{-3}), (560 K, 0.0262 Å^{-3}), and (800 K, 0.0223 Å^{-3}) for $x=0.0$, 0.2, and 0.5, respectively. The densities were determined from the zero-pressure condition. Using the Nosé-Hoover thermostat technique,[27] the equations of motion were solved via explicit reversible integrators[28] with a time step of $\Delta t=3.6$ fs. The quantities of interest were obtained by averaging over about 30 ps after an initial equilibration taking about 10 ps.

III. RESULTS

A. Structure factors

Figure 1 shows the structure factors $S(k)$ of liquid Rb_xSe_{1-x}. For $x=0.2$ and 0.5, $S(k)$ were obtained from the partial structure factors $S_{\alpha\beta}(k)$, shown in Fig. 2, with the neutron scattering lengths. In Fig. 1, the calculated results (solid lines) are compared with the experimental results[22,29,30] (open and solid circles). We are unaware of experiments for the 50% Rb concentration. It is confirmed from this figure that the calculated results are in reasonably good agreement with experiments for $x \leqslant 0.2$. In particular, the prepeak at about 1.3 Å^{-1} is reproduced very well by our calculations for $x=0.2$, which means that the system size is large enough to simulate intermediate structures indicated by the prepeak. It is seen that the prepeak grows to a clear peak at the equiatomic concentration. Such a first sharp diffraction peak has also been observed in liquid $K_{0.5}Te_{0.5}$ by neutron diffraction measurements.[13]

The Ashcroft-Langreth partial structure factors $S_{\alpha\beta}(k)$ are shown in Fig. 2. Both $S_{\mathrm{SeSe}}(k)$ and $S_{\mathrm{RbRb}}(k)$ have peaks at the wave vector 1.3 Å^{-1} at which the prepeak appears in $S(k)$. These peaks become higher and lower in $S_{\mathrm{SeSe}}(k)$ and $S_{\mathrm{RbRb}}(k)$, respectively, when x is increased from 0.2 to 0.5. In $S_{\mathrm{RbSe}}(k)$, there exists a dip at the same wave vector. It is

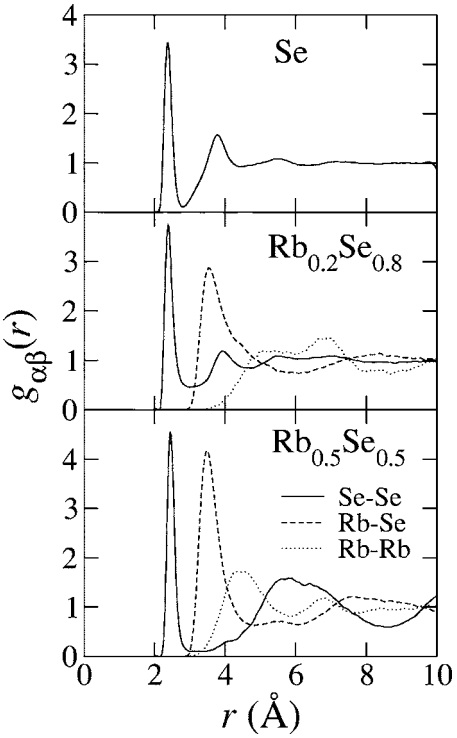

FIG. 3. Partial pair distribution functions $g_{\alpha\beta}(r)$ of liquid Rb_xSe_{1-x}. The solid, dashed, and dotted lines show $g_{\mathrm{SeSe}}(r)$, $g_{\mathrm{RbSe}}(r)$, and $g_{\mathrm{RbRb}}(r)$, respectively.

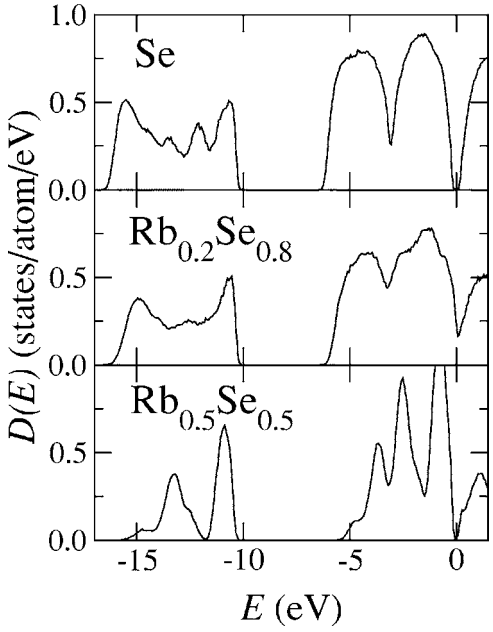

FIG. 4. Electronic densities of states $D(E)$ of liquid Rb_xSe_{1-x}. The origin of energy is taken to be the Fermi level (E_F=0).

obvious that the peaks and dips at 1.3 $Å^{-1}$ arise from charge ordering in the liquid alkali-metal–Se mixtures as in the liquid alkali-metal–Te mixtures.[16,17]

B. Pair distribution functions

Figure 3 shows the partial pair distribution functions $g_{\alpha\beta}(r)$ of liquid Rb_xSe_{1-x}. In pure liquid Se, the first peak of $g_{SeSe}(r)$ at about 2.3 Å corresponds to the correlation between the nearest neighbors within a chain, while the second peak at about 3.8 Å is mainly contributed by the next-nearest neighbors within a chain. Atomic correlations between distinct chains have also some contribution to $g_{SeSe}(r)$ beyond 3 Å.The clear minimum at about 2.8 Å indicates that Se chains do not frequently interact with each other. In $g_{SeSe}(r)$ of liquid $Rb_{0.2}Se_{0.8}$, the minimum becomes shallower, and the second peak shifts slightly toward larger r compared with that in pure liquid Se, while the position of the first peak remains the same. These changes suggest an increase of interchain interaction by the addition of Rb atoms. $g_{RbSe}(r)$ has a clear first peak at about 3.5 Å followed by a broad profile with a very shallow minimum at about 6 Å. In $g_{RbRb}(r)$, there are no clear peaks because of the low Rb concentration. When the concentration is increased to x=0.5, the profile of $g_{SeSe}(r)$ becomes very different from those at x=0.0 and 0.2, i.e., there exists a wide deep valley between the sharp first peak and the wide-ranging second peak at about 6 Å. The first peak in $g_{RbSe}(r)$ becomes sharper, while its position is unchanged. There appears a broad first peak at about 4.5 Å in $g_{RbRb}(r)$.

C. Electronic densities of states

Figure 4 shows the electronic densities of states $D(E)$ of liquid Rb_xSe_{1-x}. The origin of energy is taken to be the Fermi level. At x=0.0, $D(E)$ has a deep dip at the Fermi level corresponding to the semiconducting properties of liquid Se. With increasing alkali-metal concentration to x=0.2, the dip at the Fermi level becomes shallower, which means that the liquid has semimetallic properties, consistent with the observed concentration dependence of the electrical conductivity.[19,20] When the alkali-metal concentration is increased further (x=0.5), the dip at the Fermi level becomes deeper again. In this way, the electronic properties of the liquid alkali-metal–Se mixtures change with alkali-metal concentration: semiconducting, semimetallic, and semiconducting at x=0.0, 0.2, and 0.5, respectively.

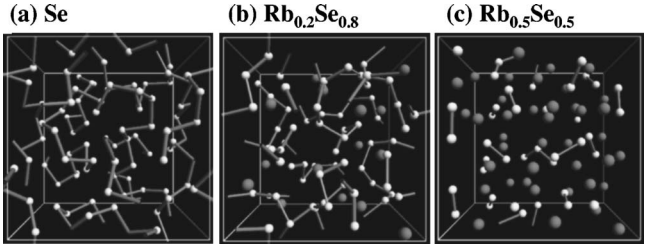

FIG. 5. Spatial configurations of atoms in liquid Rb_xSe_{1-x} for x= (a) 0.0, (b) 0.2, and (c) 0.5. The white and gray balls show the positions of Se and Rb atoms, respectively, in the supercell. The bonds connect two Se atoms with atomic distances less than 2.8 Å.

D. Spatial configurations of atoms

The spatial configurations of atoms in liquid Rb_xSe_{1-x} are shown in Fig. 5. The white and gray balls show the positions of Se and Rb atoms, respectively. It is clearly displayed that pure liquid Se consists of chain molecules. We see that the chain structure is retained at the Rb concentration of 0.2. From the time evolution of the atomic configuration, it is recognized that bond-breaking and bond-switching reactions happen more frequently on the addition of Rb atoms, which is consistent with the observations in $g_{SeSe}(r)$. At 50% Rb concentration, it is found that most Se atoms form Se_2 dimers.

E. Coordination-number distributions

To investigate the atomic coordination around Se atoms in more detail, we obtained the ratio $P(n)$ of the number of Se

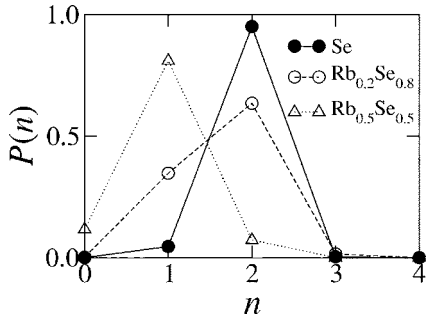

FIG. 6. Se-Se coordination-number distributions $P(n)$ of liquid Rb_xSe_{1-x}. The solid circles, open circles, and open triangles show $P(n)$ for x=0.0, 0.2, and 0.5, respectively.

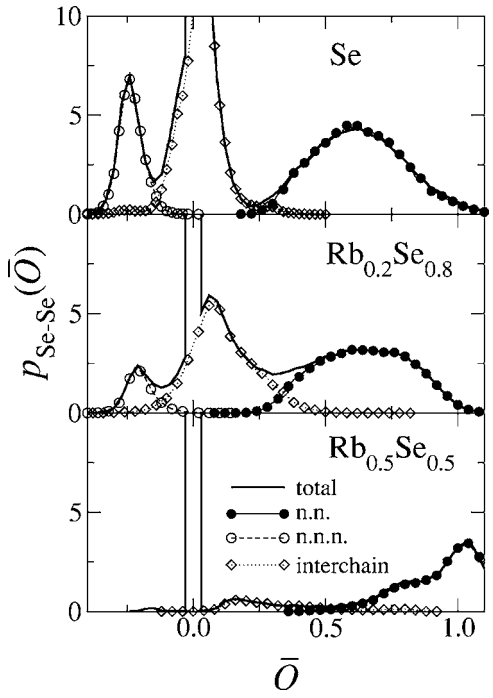

FIG. 7. Distributions $p_{\mathrm{SeSe}}(\bar{O})$ of overlap populations $O_{i\in \mathrm{Se},j\in \mathrm{Se}}$. The bold solid lines show $p_{\mathrm{SeSe}}(\bar{O})$. The solid and open circles show the contributions to $p_{\mathrm{SeSe}}(\bar{O})$ from the nearest-neighbor (n.n.) atoms and the next-nearest-neighbor (n.n.n.) atoms, respectively, within a chain, while the open diamonds show the interchain contribution to $p_{\mathrm{SeSe}}(\bar{O})$.

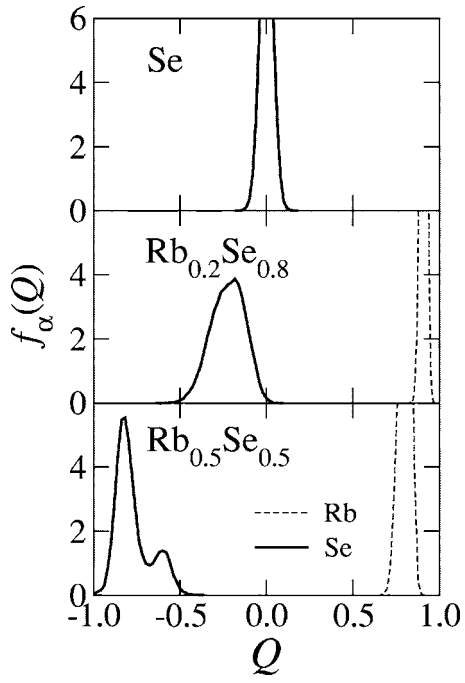

FIG. 8. Distributions $f_\alpha(Q)$ of gross charges $Q_{i\in\alpha}$. The solid and dashed lines show $f_{\mathrm{Se}}(Q)$ and $f_{\mathrm{Rb}}(Q)$, respectively.

atoms coordinated with n Se atoms to the total number of Se atoms by counting the number of atoms inside the sphere of a radius R centered at each atom. We used the first minimum position, 2.8 Å, of $g_{\mathrm{SeSe}}(r)$ as the radius R. The Rb-concentration dependence of $P(n)$ is shown in Fig. 6. It is seen that almost all Se atoms have twofold coordination in pure liquid Se. With increasing Rb concentration, twofold-coordinated Se atoms decrease, and onefold-coordinated Se atoms increase. This concentration dependence clearly shows that Se chains are shortened by the addition of alkali metals. At the Rb concentration of 50%, $P(n)$ has a large peak at $n=1$, which is consistent with the formation of Se_2 dimers.

F. Bond-overlap populations

To clarify the change in the bonding properties between Se atoms due to the addition of alkali metals, we used population analysis[31,32] by expanding the electronic wave functions in an atomic-orbital basis set.[33,34] Based on the formulation for the ultrasoft pseudopotentials,[35] we calculated the overlap population O_{ij} between the ith and jth atoms and the gross charge Q_i for the ith atom.[31] It should be noted that, since the atomic-orbital basis used in the expansion of the wave functions is not unique, a different set of atomic-orbital bases would give different values for O_{ij} and Q_i.[34] However, their relative magnitudes can be discussed meaningfully, because the trends are the same for any choice of atomic-orbital basis sets. For the basis used in our calculations, the charge spillage[33] defining the error in the expansion is less than 0.3%.

Figure 7 shows the time-averaged distributions $p_{\mathrm{SeSe}}(\bar{O})$ of the overlap populations $O_{i\in \mathrm{Se},j\in \mathrm{Se}}$ which give a semiquantitative estimate of the strength of covalentlike bonding between Se atoms. Note that the integration of $p_{\mathrm{SeSe}}(\bar{O})$, $\int_{O_{\min}}^{\infty} p_{\mathrm{SeSe}}(\bar{O})d\bar{O}$, gives the average number of Se atoms that have overlap populations greater than $O_{\min}$ around one Se atom. For the Rb concentrations for $x\leqslant 0.2$, $p_{\mathrm{SeSe}}(\bar{O})$ consists mainly of three peaks at about $\bar{O}=0.7$, 0.1, and −0.2 as shown by the solid lines for liquid Se and liquid $Rb_{0.2}Se_{0.8}$ in Fig. 7. Note that there is a large peak at $\bar{O}=0.0$, because we calculated O_{ij} for pairs of Se atoms with a large cutoff distance (~7 Å) so as to take into account all pairs of Se atoms chemically interacting with each other. Finite values of O_{ij} are obtained for Se pairs with atomic distances up to about 5 Å. O_{ij} obtained for pairs with further atomic distances are nearly zero, and give the peak at $\bar{O}=0.0$.

To examine $p_{\mathrm{SeSe}}(\bar{O})$ in connection with the chain structure of Se atoms, we identified Se chains in the liquid mixtures by connecting up Se atoms with atomic distances less than 2.8 Å, the minimum position of $g_{\mathrm{SeSe}}(r)$. Since each Se atom is assigned to one of the chains, we can specify the spatial relation between two Se atoms selected arbitrarily with respect to the chain structure. The solid circles in Fig. 7 show the time-averaged distributions of the overlap populations for pairs of Se atoms that are nearest neighbors to each other within a chain. Each Se atom is connected to its nearest neighbors by a σ-type bond, and the distributions have peaks at the larger $\bar{O}\sim 0.7$. Pairs of Se atoms that are next-nearest neighbors to each other within a chain give the time-

averaged distributions displayed by the open circles in Fig. 7. Because of the antibonding interaction between the lone-pair states, the distributions have peaks at the negative $\bar{O} \sim -0.2$. The distributions shown by the diamonds in Fig. 7 are given by pairs of Se atoms belonging to different chains. Since the interchain interaction is weak, the peaks exist at the smaller $\bar{O} \sim 0.1$.

It is seen in pure liquid Se that the distributions shown by the solid circles and the diamonds are well separated by a clear minimum at about $\bar{O}=0.2$, and that the next-nearest-neighbor Se atoms give a large peak at about $\bar{O}=-0.2$ (open circles). These features reflect the existence of Se molecules that have a clear chain structure. At the Rb concentration of 0.2, the distribution by the interchain interaction (diamonds) spreads over larger overlap populations, and the minimum at about $\bar{O}=0.2$ becomes shallower, which indicates that Se chains interact more frequently with each other due to the excess electronic charges transferred from Rb atoms. Also the height of the peak at $\bar{O}=-0.2$ becomes lower. These facts are consistent with the shortening of chains. At the equiatomic concentration, $p_{\mathrm{SeSe}}(\bar{O})$ has a qualitatively different distribution from those at the lower Rb concentrations, reflecting the formation of dimers. The distribution shown by the solid circles shifts to larger overlap populations, and has a peak at about $\bar{O}=1.0$, which shows a stronger chemical bonding in dimers. The distribution by the interchain interaction (diamonds) has a profile spreading over a wide range of $\bar{O}$ with a very low peak, which indicates that the dimer-dimer interaction occurs infrequently.

G. Mulliken charges

Figure 8 shows the time-averaged distributions $f_\alpha(Q)$ of $Q_{i\in\alpha}$ for α-type atoms. Note that $f_\alpha(Q)$ is normalized as $\int f_\alpha(Q)dQ=1$. In pure liquid Se, $f_{\mathrm{Se}}(Q)$ naturally has a symmetric distribution around $Q=0.0$. In liquid $\mathrm{Rb}_x\mathrm{Se}_{1-x}$ for $x=0.2$ and 0.5, $f_{\mathrm{Rb}}(Q)$ has peaks near $Q=1.0$, which reflects the fact that almost all $5s$ electrons of Rb atoms are transferred to Se atoms. At $x=0.2$, $f_{\mathrm{Se}}(Q)$ has an asymmetric distribution with the peak at about $Q=-0.2$. The asymmetry comes from the coordination dependence of the gross charges, i.e., onefold-coordinated Se atoms have more electrons than twofold-coordinated Se atoms. At $x=0.5$, $f_{\mathrm{Se}}(Q)$ has two peaks; the high peak at about $Q=-0.8$ is given by Se atoms in stable dimers, while the small peak at about $Q=-0.6$ arises from rearrangements of dimers. When two dimers interact with each other, a short chain is formed transiently, and Se atoms have fewer electrons

IV. DISCUSSION

Here, we discuss the effects of alkali metals on the electronic and structural properties of the liquid alkali-metals–Se mixtures in comparison with the liquid alkali-metals–Te mixtures. As seen in the spatial configurations of atoms (Fig. 5) and the coordination-number distributions (Fig. 6), Se chains are shortened by the addition of Rb atoms in liquid $\mathrm{Rb}_x\mathrm{Se}_{1-x}$. The electronic densities of states (Fig. 4) show that the electronic properties of liquid $\mathrm{Rb}_{0.2}\mathrm{Se}_{0.8}$ are semimetallic, while pure liquid Se has semiconducting properties. The distributions of the overlap populations (Fig. 7) and the gross charges (Fig. 8) clearly show that $5s$ electrons of Rb atoms are transferred almost completely to Se atoms, and that the transferred electrons enhance the interchain interaction at $x=0.2$.

On the other hand, in pure liquid Te, there exist many threefold-coordinated Te atoms.[7–9] The Te-Te coordination distribution[16] shows that twofold- and threefold-coordinated Te atoms exist in almost the same percentage. By adding alkali metals, threefold-coordinated Te atoms decrease, and twofold-coordinated Te atoms increase, which means that the chain structure is stabilized, in contrast to the liquid alkali-metals–Se mixtures. The calculated electronic densities of states[16,17] have revealed that liquid Te has semimetallic properties, and that the electronic properties become semiconducting with increasing alkali-metal concentration reflecting the stabilization of Te chains.

The distribution of overlap populations $p_{\mathrm{TeTe}}(\bar{O})$ for pure liquid Te has a broad profile, and has no clear peak (except for $\bar{O}=0.0$),[35] which is consistent with the existence of many threefold-coordination defects. This indicates that bond breaking and bond exchange occur much more frequently compared with those in pure liquid Se, and that the σ-type bonding between Te atoms is weaker than that between Se atoms. By the addition of alkali metals, the transferred electrons function to make the Te-Te bonding stronger, and stabilize the chain structure.

From these observations, we see that the role of the transferred electrons in liquid alkali-metal chalcogenides depends on the spatial localization of electrons in pure liquid chalcogens. Liquid Se has a well-localized electron distribution in the chain structure, i.e., four p electrons of each Se atom occupy the σ-type bonding and lone-pair nonbonding states around the Se atom. Since the σ^*-type antibonding states are well separated energetically from these occupied states, the bond breaking and bond exchange scarcely take place in liquid Se. When alkali metals are added, the transferred electrons probably occupy the σ^*-type antibonding states, because the bonding and nonbonding states are already occupied. Due to the antibonding character of the electronic states occupied by the transferred electrons, Se-Se bonds become weaker, and the interaction between Se chains is enhanced. In contrast, the valence electrons are distributed over the chains in pure liquid Te as it has metallic properties. Considering the fact that bond breaking and bond exchange occur frequently, the electronic states in liquid Te have antibonding character as well as bonding and nonbonding characters. In other words, the bonding and nonbonding states around Te chains are partially occupied. If extra electrons are given by the addition of alkali metals, those bonding and nonbonding electronic states are preferentially occupied by the electrons so as to make the chain structure stable. It is noted that, at the equiatomic concentration, almost all chalcogen atoms form divalent anion dimers in both the liquid alkali-metal–Te and alkali-metal–Se mixtures.

V. SUMMARY

We have investigated the structure and electronic states of liquid Rb_xSe_{1-x} by means of *ab initio* molecular-dynamics simulations. It has been shown that the calculated structure factors are in reasonable agreement with experiments. We have confirmed from the calculated electronic densities of states that the electronic properties of the liquid alkali-metal–Se mixtures change from semiconducting to semimetallic with increasing alkali-metal concentration from $x=0.0$ to 0.2. The shortening of Se chains occurs due to the transferred electrons, and is responsible for the metallic properties. Based on the population analysis, we have discussed the effects of the transferred electrons on the chain structure in connection with the bonding properties in liquid Se and liquid Te.

ACKNOWLEDGMENTS

The authors acknowledge K. Maruyama, H. Hoshino, and H. Endo for providing us with their experimental data. They are grateful to M. Aniya for useful discussions. The present work was supported in part by a Grant-in-Aid for Scientific Research on Priority Area "Nanoionics (439)," and a Grant-in-Aid for Scientific Research (C) by the Ministry of Education, Culture, Sports, Science and Technology of Japan. The authors thank the Supercomputer Center, Institute for Solid State Physics, University of Tokyo for the use of the facilities.

[1] *The Physics of Selenium and Tellurium*, Proceedings of the International Conference on the Physics of Selenium and Tellurium, Königstein, Germany, 1979, edited by E. Gerlach and P. Grosse (Springer, Berlin, 1979).
[2] J. C. Perron, J. Rabit, and J. F. Rialland, Philos. Mag. B **46**, 321 (1982).
[3] W. Freyland and M. Cutler, J. Chem. Soc., Faraday Trans. 2 **176**, 756 (1980).
[4] H. Hoshino, R. W. Schmutzler, and F. Hensel, Ber. Bunsenges. Phys. Chem. **80**, 27 (1976).
[5] H. Hoshino, R. W. Schmutzler, W. W. Warren, Jr., and F. Hensel, Philos. Mag. **33**, 255 (1976).
[6] F. Shimojo, K. Hoshino, M. Watabe, and Y. Zempo, J. Phys.: Condens. Matter **10**, 1199 (1998).
[7] S. Takeda, S. Tamaki, and Y. Waseda, J. Phys. Soc. Jpn. **53**, 3830 (1984).
[8] A. Munelle, R. Bellissent, and A. M. Frank, Physica B **156**, 174 (1989).
[9] T. Tsuzuki, M. Yao, and H. Endo, J. Phys. Soc. Jpn. **64**, 485 (1995).
[10] C. A. Kraus and S. W. Glass, J. Phys. Chem. **33**, 984 (1929).
[11] M.-L. Saboungi, J. Fortner, J. W. Richardson, A. Petric, M. Doyle, and J. E. Enderby, J. Non-Cryst. Solids **156-158**, 356 (1993).
[12] Y. Kawakita, M. Yao, H. Endo, and J. Dong, J. Non-Cryst. Solids **205-207**, 447 (1996).
[13] J. Fortner, M. -L. Saboungi, and J. E. Enderby, Phys. Rev. Lett. **69**, 1415 (1992).
[14] Y. Kawakita, J. Dong, T. Tsuzuki, Y. Ohmasa, M. Yao, H. Endo, H. Hoshino, and M. Inui, J. Non-Cryst. Solids **156-158**, 756 (1993).
[15] Y. Kawakita, M. Yao, and H. Endo, J. Phys. Soc. Jpn. **66**, 1339 (1997).
[16] F. Shimojo, K. Hoshino, and Y. Zempo, Phys. Rev. B **59**, 3514 (1999).
[17] F. Shimojo, K. Hoshino, and Y. Zempo, Phys. Rev. B **63**, 094206 (2001).
[18] J. Hafner, K. Seifert-Lorentz, and O. Genser, J. Non-Cryst. Solids **250-252**, 225 (1999).
[19] S. Hosokawa, M. Yao, T. Yoshimura, and H. Endo, J. Phys. Soc. Jpn. **54**, 4717 (1985).
[20] H. Hoshino and H. Endo, J. Non-Cryst. Solids **117-118**, 525 (1990).
[21] K. Maruyama, H. Hoshino, H. Endo, M. Yamazaki, and T Miyanaga, J. Phys.: Condens. Matter **17**, S3317 (2005).
[22] K. Maruyama, H. Endo, and H. Hoshino, J. Phys. Soc. Jpn. **74**, 3213 (2005).
[23] J. P. Perdew, K. Burke, and M. Ernzerhof, Phys. Rev. Lett. **77**, 3865 (1996).
[24] G. Kresse and J. Hafner, Phys. Rev. B **49**, 14251 (1994).
[25] F. Shimojo, R. K. Kalia, A. Nakano, and P. Vashishta, Comput. Phys. Commun. **140**, 303 (2001).
[26] D. Vanderbilt, Phys. Rev. B **41**, 7892 (1990).
[27] S. Nosé, Mol. Phys. **52**, 255 (1984); W. G. Hoover, Phys. Rev. A **31**, 1695 (1985).
[28] M. Tuckerman, B. J. Berne, and G. J. Martyna, J. Chem. Phys. **97**, 1990 (1992).
[29] K. Tamura and S. Hosokawa, Ber. Bunsenges. Phys. Chem. **96**, 681 (1992).
[30] K. Tamura and M. Inui, J. Phys.: Condens. Matter **13**, R337 (2001).
[31] R. S. Mulliken, J. Chem. Phys. **23**, 1833 (1955).
[32] R. S. Mulliken, J. Chem. Phys. **23**, 1841 (1955).
[33] D. Sánchez-Portal, E. Artacho, and J. M. Soler, J. Phys.: Condens. Matter **8**, 3859 (1996).
[34] M. D. Segall, R. Shah, C. J. Pickard, and M. C. Payne, Phys. Rev. B **54**, 16317 (1996).
[35] F. Shimojo, K. Hoshino, and Y. Zempo, J. Phys. Soc. Jpn. **72**, 2822 (2003).